



HAL
open science

Cooperative emission of a coherent superflash of light

Chang Chi Kwong, Tao Yang, Mysore S. Pramod, Kanhayia Pandey,
Dominique Delande, Romain Pierrat, David Wilkowski

► **To cite this version:**

Chang Chi Kwong, Tao Yang, Mysore S. Pramod, Kanhayia Pandey, Dominique Delande, et al..
Cooperative emission of a coherent superflash of light. 2014. hal-00994145v1

HAL Id: hal-00994145

<https://hal.science/hal-00994145v1>

Preprint submitted on 21 May 2014 (v1), last revised 4 Dec 2014 (v2)

HAL is a multi-disciplinary open access archive for the deposit and dissemination of scientific research documents, whether they are published or not. The documents may come from teaching and research institutions in France or abroad, or from public or private research centers.

L'archive ouverte pluridisciplinaire **HAL**, est destinée au dépôt et à la diffusion de documents scientifiques de niveau recherche, publiés ou non, émanant des établissements d'enseignement et de recherche français ou étrangers, des laboratoires publics ou privés.

Cooperative emission of a coherent superflash of light

C. C. Kwong,¹ T. Yang,² M. S. Pramod,² K. Pandey,² D. Delande,³ R. Pierrat,⁴ and D. Wilkowski^{1,2,5}

¹*School of Physical and Mathematical Sciences, Nanyang Technological University, 637371 Singapore, Singapore*

²*Centre for Quantum Technologies, National University of Singapore, 117543 Singapore, Singapore*

³*Laboratoire Kastler Brossel, UPMC-Paris 6, ENS, CNRS; 4 Place Jussieu, 75005 Paris, France*

⁴*ESPCI ParisTech, PSL Research University, CNRS,*

Institut Langevin, 1 rue Jussieu, F-75005, Paris, France

⁵*Institut Non Linéaire de Nice, Université de Nice Sophia-Antipolis, CNRS UMR 7335, 06560 Valbonne, France*

(Dated: May 21, 2014)

We investigate the transient coherent transmission of light through an optically thick cold strontium gas. We observe a coherent superflash just after an abrupt probe extinction, with peak intensity more than 3 times the incident one. We show that this coherent superflash is a direct signature of the cooperative forward scattering emission of the atoms induced by the probe in the stationary regime. Thus, surprisingly we find that the forward scattering amplitude can be larger than the incident probe excitation amplitude. By engineering fast transient phenomena on the incident field, we give a clear and simple picture of the physical mechanisms at play.

PACS numbers: 42.50.Md, 42.25.Dd

We consider a simple scheme where a laser beam is sent through a slab uniformly filled with resonant point-like scatterers. In the stationary regime, scattering leads to an attenuation of the intensity, $I_t = |E_t|^2$, of the transmitted coherent field E_t , according to the Beer-Lambert law:

$$I_t = I_0 \exp(-b), \quad (1)$$

where I_0 is the intensity of the incident field E_0 and b is the optical thickness of the medium. The power lost in the coherent transmission, $\propto 1 - e^{-b}$, leaves the medium in all directions [1, 2]. In general, since the positions of the scatterers are random, the re-emitted field is incoherent (i.e. the phase of the incident field is lost). This statement is, however, not true in the forward direction, where the phase of the scattered field does not depend on the (transverse) positions of the scatterers [3]. This cooperative effect of the atomic ensemble in the forward direction has already been explored by several authors, for example in superradiance laser [4, 5], superradiance of a single photon emission [6], and in the underlying mechanical effects on the atomic cloud [7]. Importantly, the attenuation of the transmitted field can be interpreted as the result of a destructive interference between the incident field and the field scattered in the forward direction. Denoting by E_s the forward scattered electric field, one has at any time

$$E_t = E_0 + E_s. \quad (2)$$

For the useful case of a monochromatic fields at frequency ω in the stationary regime, such an equality can be written for the *complex* field amplitudes [see Fig. 1(a) for a geometrical reconstruction]. In general, the fields have two polarization components perpendicular to the direction of propagation, so vectors should be used. We here

consider a simpler situation where all fields have the same polarization.

Measuring the forward scattered electric field and its interference properties with the incident field is the major goal of our work. In the stationary regime, energy conservation imposes $I_t \leq I_0$. In other words, $|E_t| \leq |E_0|$ and therefore $|E_s| \leq 2|E_0|$. However, since the forward scattered field is built upon the incident field, one might believe that its amplitude is bounded as such, $|E_s| \leq |E_0|$. As a key result of this letter, we show that the latter intuitive picture is incorrect. We indeed predict a forward scattered intensity I_s arbitrarily close to $4I_0$ and experimentally observe $I_s/I_0 = 3.1(4)$. The experimental value is mainly limited by the temperature of the gas and the maximum optical thickness that can be obtained with our experimental setup. Hence, apart from the energy conservation argument, we find no other basic principles or theorems, such as causality or Kramers-Kronig relations, that limit the amplitude of the forward scattered field.

The system under investigation consists of a laser-cooled ^{88}Sr atomic gas. The details of the cold atoms production line are given in Ref. [8]. The last cooling stage is performed on the $^1S_0 \rightarrow ^3P_1$ intercombination line at $\lambda = 689$ nm, with a bare linewidth of $\Gamma/2\pi = 7.5$ kHz. The number of atoms is $2.5(5) \times 10^8$. The temperature of the cold gas is $T = 3.3(2)$ μK , corresponding to an *rms* velocity of $\bar{v} = 3.4\Gamma/k$. Here, $k = 2\pi/\lambda$ is the wavevector of the transition. After cooling, the atomic cloud is expanded in the dark for 10 ms. The peak density is then around $\rho = 4.6 \times 10^{11}$ cm^{-3} . The cloud has an oblate ellipsoidal shape with an axial radius 240(10) μm and an equatorial radius 380(30) μm . Using shadow imaging technique, we measure along an equatorial direction of the cloud, an optical thickness at resonance of $b_0 = 19(3)$ on the intercombination line. We

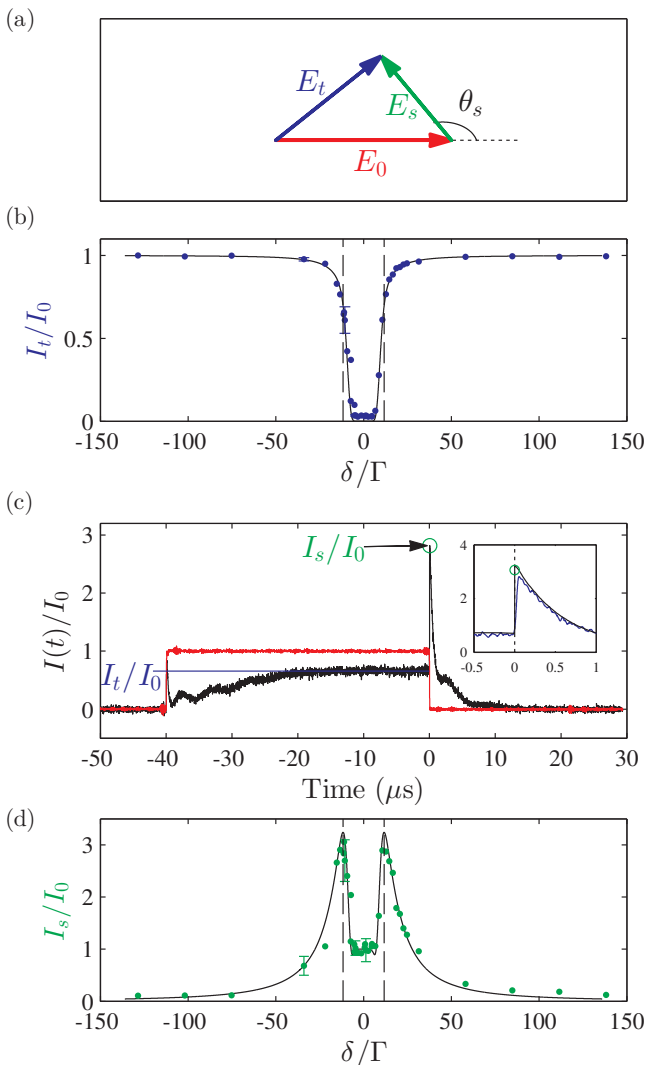


Figure 1: (Color online) (a) Electric fields in the complex plane. (b) I_t/I_0 in the stationary regime as a function of the probe detuning δ/Γ . The blue dots are the experimental data and the black solid line is the theoretical prediction. (c) Example of a temporal evolution of the normalized transmitted intensity for $\delta = -11.2\Gamma$. The red curve shows the normalized incident intensity, the black curve shows the experimental signal, the blue line shows the level of I_t/I_0 and the green open circle shows the value of I_s/I_0 . The inset panel is a zoom around $t = 0$ of the coherent superflash, the black curve showing the theoretical prediction assuming instantaneous switch off of the probe. (d) I_s/I_0 in the stationary regime as a function of the probe detuning. The black solid line is the theoretical prediction and the green dots are the experimental data. The vertical dashed lines at $|\delta| = 11.7\Gamma$ in (b) and (d) define the expected positions of the maximum values of the forward scattered intensity. In the experiment, $T = 3.3(2) \mu\text{K}$ and $b_0 = 19(3)$, the other parameters being given in the text.

note that $k\ell \simeq 500$, where ℓ is the light scattering mean free path. Since $k\ell \gg 1$, the system is deeply in the

dilute regime. Hence, all collective behaviors such as recurrent scattering [9, 10], Lorentz-Lorenz and collective Lamb shift [11–13], can be disregarded.

A probe laser beam is then sent across the cold atomic gas along an equatorial axis. The probe (diameter $150 \mu\text{m}$) is tuned around the resonance of the intercombination line. Its power is $400(40) \text{ pW}$, corresponding to $0.45(5)I_{\text{sat}}$, where $I_{\text{sat}} = 3 \mu\text{W}/\text{cm}^2$ is the saturation intensity of the transition. The probe is switched on for $40 \mu\text{s}$ such that the stationary regime is reached without introducing significant radiation pressure on the atoms. The same probe sequence is repeated 1 ms later without the atoms to measure I_0 . The temporal evolution of I_t is measured using an amplified photodetector (Hamamatsu, model C10508, cut-off frequency: 10 MHz). All the transmitted photons along the propagation direction are collected, leading to a transverse integration of the intensity. During probing, we apply a bias magnetic field of 1.4 G along the beam polarization to address a two-level system corresponding to the $^1S_0, m = 0 \rightarrow ^3P_1, m = 0$ transition.

We first look at the stationary regime. We plot in Fig. 1(b) I_t/I_0 as a function of the probe frequency detuning. In order to compare with analytical predictions, we model the ellipsoid geometry of the cloud by a slab geometry. In the frequency domain, the coherent transmitted electric field through the slab is given by

$$E_t(\omega) = E_0(\omega) \exp \left[i \frac{n(\omega)\omega L}{2c} \right]. \quad (3)$$

We define, $n(\omega)$, ω , c and L , respectively as the complex refractive index, the laser optical frequency, the speed of light in vacuum and the thickness of the slab along the laser beam. For a dilute medium, we have $n(\omega) = 1 + \rho\alpha(\omega)/2$ [14]. The two-level atomic polarizability is given by

$$\alpha(\omega) = -\frac{3\pi\Gamma c^3}{\omega^3} \frac{1}{\sqrt{2\pi}\bar{v}} \int_{-\infty}^{+\infty} dv \frac{\exp(-v^2/2\bar{v}^2)}{\delta - kv + i\Gamma/2}, \quad (4)$$

where the integration is carried out over the thermal Gaussian distribution of the atomic velocity along the beam propagation direction. $\delta = \omega - \omega_0$ is the frequency detuning and ω_0 is the bare atomic transition frequency. By inserting in Eqs. (3) and (4) the measured values of the atomic density and the temperature, we compute the transmitted intensity I_t and show the results in Fig. 1(b). The effective slab thickness of the cloud is chosen to match the measured optical thickness. The theoretical prediction agrees very well with the experimental data. However, close to resonance, the measured transmission is slightly higher than the predicted one. This mismatch is due to the finite transverse size of the cloud, which allows few photons in the wings of the laser beam to be directly transmitted.

We now take advantage of the finite response time of the atom/light system to measure directly the forward scattered intensity. For this purpose, we abruptly switch off the probe beam. The switching time is 40 ns (i.e. ~ 500 times faster than the excited state lifetime $\Gamma^{-1} = 21 \mu\text{s}$). According to Eq. (2), if $I_0 = 0$, we have $E_t(t = 0^+) = E_s$. Hence, immediately after switching off the probe, the detector measures the forward scattered intensity of the stationary regime (i.e. $I_t(t = 0^+) = I_s$). In the absence of a driving incident field, the transmitted intensity decays because of the natural decay of the atomic dipoles, but also because of the dephasing induced by propagation in an optically thick medium and Doppler broadening [15]. This phenomenon is known as the free induction decay. It has been initially studied in NMR [16] and more recently in optics with cold atomic gases [17–20]. If the probe is at resonance and the optical thickness is large, the free induction decay leads to the emission of a coherent flash of light with a peak intensity equals to I_0 (see for example Fig. 1(b) in Ref. [15]). For a detuned probe field, one illustrative example of the temporal evolution of I_t/I_0 is given in Fig. 1(c). In this case, we observe a flash of light with the peak intensity clearly above I_0 . We define it as a coherent superflash. This is in contrast with the coherent flash at an intensity below or equal to I_0 reported in Ref. [15]. In the inset of Fig. 1(c), we compare the experimental signal and the theoretical prediction. This theoretical prediction is obtained by numerically calculating the inverse Fourier transform of Eq. 3 for an incident field that is a step function in the time domain. A good agreement is obtained, except at $t = 0$, where the finite response time of our detection scheme slightly smoothes the predicted discontinuity. The value of I_s is obtained by extrapolating the (super)flash down to $t = 0$.

We plot in Fig. 1(d) the normalized forward scattered intensity in the stationary regime as a function of the laser detuning. At resonance, we find $I_s/I_0 \simeq 1$ and $I_t/I_0 \simeq 0$, like in Ref. [15], meaning that the interference between the incident field and the forward scattered field is almost perfectly destructive (i.e. $E_s \simeq -E_0$). Far from resonance, $I_s \xrightarrow{|\delta| \rightarrow \infty} 0$ so that $I_t \xrightarrow{|\delta| \rightarrow \infty} I_0$. In between these two extreme cases, I_s/I_0 passes through a maximum of 3.1(4) at $|\delta| = 11.2(7)\Gamma$. At the same absolute value of the detuning, we get $I_t/I_0 = 0.66(8)$. Finding $I_s > I_0$ (i.e. a coherent superflash) is surprising for two reasons. First, as mentioned earlier, the forward scattered field is built upon the incident field. Second, it reaches its maximum value when the field is mostly transmitted (i.e. where we could expect that the incident field weakly interacts with the medium).

Using Eqs. (2) and (3), we find the maximum value of I_s/I_0 to be 4. We tend to this limit as we increase the optical thickness, as shown in Fig. 2. For $|\delta| \gg k\bar{v}$, the maximum superflash intensity at a given large b_0 occurs for $\theta_s = \pi$. Using Eqs. (2) and (3), we can show that this

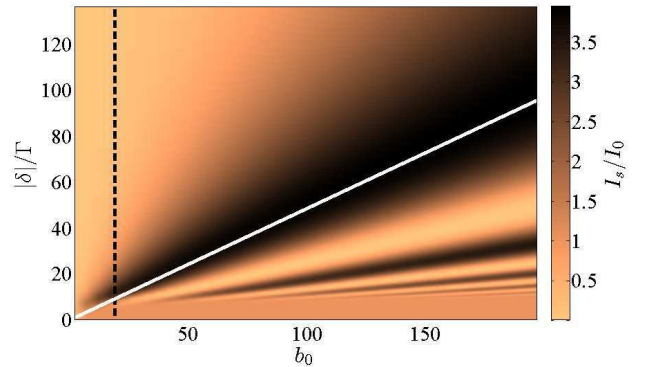


Figure 2: (Color online) Prediction for the I_s/I_0 ratio vs. parameters b_0 (optical thickness at resonance) and detuning $|\delta|/\Gamma$ for $T = 3.3(2) \mu\text{K}$. The black dashed line indicates the optical thickness of our experiment. The white solid line represents the linear dependence on b_0 of the maximum value of I_s/I_0 . A coherent superflash is emitted when $I_s/I_0 > 1$.

corresponds to [15] $|\delta|/\Gamma \approx b_0/4\pi g(k\bar{v}/\Gamma)$ where $g(x) = \sqrt{\pi/8} \exp(1/8x^2) \text{erfc}(1/\sqrt{8}x)/x$. At this detuning, the superflash intensity is $I_s/I_0 \approx 4[1 - 2\pi^2 g(k\bar{v}/\Gamma)/b_0]$. At $T = 3.3 \mu\text{K}$, the temperature of the experiment, $g(k\bar{v}/\Gamma) = 0.16$. The detuning at maximum superflash intensity is then given by $|\delta|/\Gamma \approx 0.48b_0$, a linear dependence on b_0 which can be seen in Fig. 2.

From our experimental measurements of I_t/I_0 (stationary transmitted probe intensity) and I_s/I_0 (immediately after switching off the probe), we can also extract the *phase* of the forward scattered field:

$$\theta_s = \text{acos} \left(\frac{I_t - I_0 - I_s}{2\sqrt{I_0 I_s}} \right). \quad (5)$$

However, there is an ambiguity in the phase calculated using Eq. (5), since we cannot distinguish between θ_s and $-\theta_s$. To disambiguate, the easiest way is to choose the sign giving the best agreement with Eqs. (3) and (4). This is the first procedure used in Fig. 3.

We have also added theoretical predictions in Fig. 3 and we note that the phase angle θ_s is within the range $[\pi/2, 3\pi/2]$, which means that the forward scattered field always destructively interfere with E_0 , as expected from a scattering medium. We also note that for large detunings $\theta_s \xrightarrow{|\delta| \rightarrow \pm\infty} \mp \pi/2$. However, $|E_s|$ is close to zero so E_s stays close to the origin. As the detuning decreases, E_s traces a curve as depicted in Fig. 3 until we reach a situation where $\theta_s \simeq \pi$. If this happens when the detuning is still relatively large, as it is in the experiment, a large superflash intensity is observed. Close to resonance, θ_s should tend to π . This measurement is however affected by a large systematic error because of the residual transmission, as discussed in Fig. 1(b).

At very large optical thickness θ_s goes back and forth in the $[\pi/2, 3\pi/2]$ range, leading to a potential observa-

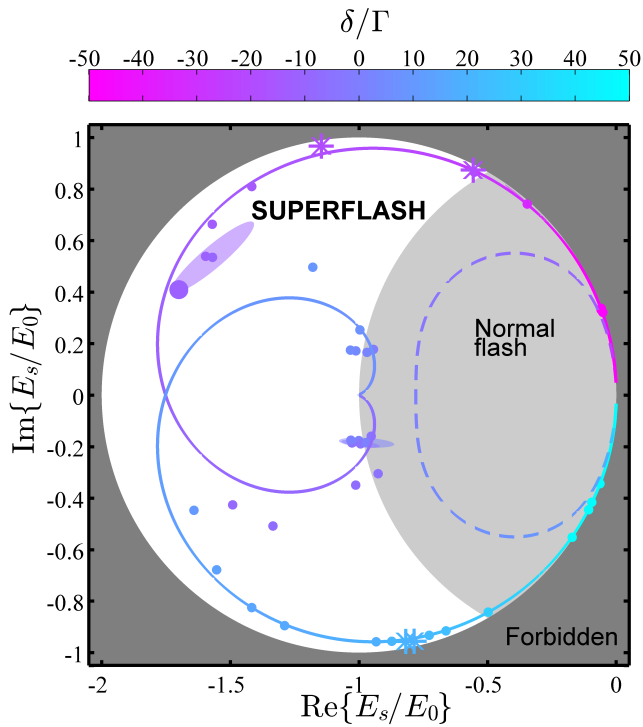


Figure 3: (Color online) Reconstruction of E_s in the complex plane. The false color scale gives the probe detuning. The white region corresponds to the superflash regime, the light gray area shows the region with the normal coherent flash and the dark gray area gives the region forbidden by energy conservation. The dots are the experimental values extracted using eq. (5) whereas the stars are experimental values obtained by abruptly changing the phase of E_0 . The transparent ellipses around several experimental data depict the error estimates. The solid curve is the theoretical prediction. The dashed curve is the theoretical prediction at a lower optical thickness ($b_0 = 3$) and same temperature $T = 3.3 \mu\text{K}$.

tion of several superflashes by scanning the detuning at a given b_0 [see Fig. 2]. At low optical thickness, the excursion of θ_s is limited and no superflash occurs as illustrated by the dash curve in Fig. 3.

An additional measurement makes it possible to disambiguate the sign of the phase θ_s . We insert, in the optical path of the probe, an electro-optic modulator (EOM) to adjust the phase delay of E_0 . We abruptly switch off a bias voltage of the EOM, while keeping the probe on. This operation creates an abrupt negative jump of the incident phase. If after the phase jump, the incident field tends to align with E_s , we observe the usual positive (super)flash [see Fig. 4(b)]. On the contrary, if E_0 points opposite to E_t , we observe a negative flash [see Fig. 4(a)]. We vary the phase jumps in the $[0, -\pi]$ range where the amplitude of the (super)flash necessarily passes through an extremum giving, without ambiguity, θ_s . We show as stars in Fig. 3 several values of the such reconstructed field. They are in good agreement with the previous ex-

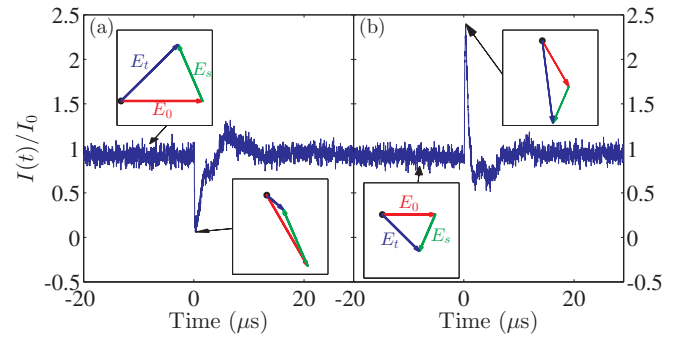


Figure 4: (Color online) Temporal evolution (blue curves) with an abrupt change of phase of -0.4π at $t = 0$ for a probe detuning of (a) $\delta = -19.3\Gamma$ and (b) $\delta = +20.7\Gamma$. The insets show the electric fields in the complex plane at the time pointed by the arrows.

perimental values represented by dots.

In conclusion, we have studied fast transient phenomena in the transmission of a probe beam through an optically thick cold atomic sample. When a probe at a detuning $|\delta|/\Gamma \approx b_0/4\pi g(k\bar{v}/\Gamma)$ is abruptly switched off, a short coherent superflash is emitted with a peak intensity up to 4 times the incident intensity. By combining transient and stationary intensity measurements, we show that at large detuning the coherent superflash comes from a phase rotation of the forward scattered field induced by the large optical thickness of the medium. Moreover, by abruptly changing the phase of the incident field, we were able to engineer positive and negative coherent flash emissions. The latter shows that an optically dense medium might be useful as a phase discriminator device. Potential applications might be found in classical and quantum information such as detection and feedback of phase, generation of squeezed states, and continuous variable entanglement.

We have used the narrow width intercombination line of Strontium as a proof-of-principle of the coherent (super)flash effect in the easily accessible nanosecond regime. However, broader transitions and larger optical thickness may considerably shorten the flash duration. It seems possible then, with a simple system, namely a CW laser, an absorber and a fast phase modulator, to generate short coherent pulses at a high repetition rate for potential applications in ultrafast physics and optical communication.

The authors are grateful to R. Carminati, C. Salomon and J. Ye for fruitful discussions. CCK thanks CQT and ESPCI institutions for funding his trip to Paris. This work was supported by the CQT/MoE funding grant No. R-710-002-016-271. RP acknowledges the support of LABEX WIFI (Laboratory of Excellence ANR-10-LABX-24) within the French Program ‘‘Investments for the Future’’ under reference ANR-10-IDEX-0001-02 PSL*.

-
- [1] A. Fioretti, A. F. Molisch, J. H. Müller, P. Verkerk, and M. Allegrini, *Opt. Commun.* **149**, 415 (1998).
- [2] G. Labeyrie, E. Vaujour, C. A. Müller, D. Delande, C. Miniatura, D. Wilkowski, and R. Kaiser, *Phys. Rev. Lett.* **91**, 223904 (2003).
- [3] Partial coherence exists in the backward direction as well. See for example, Y. Bidel *et al.*, *Phys. Rev. Lett.* **88**, 203902 (2002) and references therein.
- [4] D. Meiser, J. Ye, D. R. Carlson, and M. J. Holland, *Phys. Rev. Lett.* **102**, 163601 (2009).
- [5] J. G. Bohnet, Z. Chen, J. M. Wiener, D. Meiser, M. J. Holland, and J. K. Thompson, *Nature (London)* **484**, 78 (2012).
- [6] M. O. Scully and A. A. Svidzinsky, *Science* **325**, 1510 (2009).
- [7] T. Bienaimé, S. Bux, E. Lucioni, Ph. W. Courteille, N. Piovella, and R. Kaiser, *Phys. Rev. Lett.* **104**, 183602 (2010).
- [8] T. Yang *et al.* (unpublished).
- [9] I. M. Sokolov, M. D. Kupriyanova, D. V. Kupriyanov, and M. D. Havey, *Phys. Rev. A* **79**, 053405 (2009).
- [10] C. C. Kwong, D. Wilkowski, D. Delande, and R. Pierrat (unpublished).
- [11] J. Pellegrino, R. Bourgain, S. Jennewein, Y. R. P. Sortais, and A. Browaeys, arXiv:1402.4167.
- [12] J. Keaveney, A. Sargsyan, U. Krohn, I. G. Hughes, D. Sarkisyan, and C. S. Adams, *Phys. Rev. Lett.* **108**, 173601 (2012).
- [13] J. Javanainen, J. Ruostekoski, Y. Li, and S.-M. Yoo, *Phys. Rev. Lett.* **112**, 113603 (2014).
- [14] E. Hetch and A. Zajac, *Optics* (Addison-Wesley, Reading, MA, 1974).
- [15] M. Chalony, R. Pierrat, D. Delande, and D. Wilkowski, *Phys. Rev. A* **84**, 011401(R) (2011).
- [16] E. L. Hahn, *Phys. Rev.* **77**, 297 (1950).
- [17] K. Toyoda, Y. Takahashi, K. Ishikawa, and T. Yabuzaki, *Phys. Rev. A* **56**, 1564 (1997).
- [18] U. Shim, S. Cahn, A. Kumarakrishnan, T. Sleator, and J.-T. Kim, *Jpn. J. Appl. Phys.* **41**, 3688 (2002).
- [19] H. Jeong, A. M. C. Dawes, and D. J. Gauthier, *Phys. Rev. Lett.* **96**, 143901 (2006).
- [20] D. Wei, J. F. Chen, M. M. T. Loy, G. K. L. Wong, and S. Du, *Phys. Rev. Lett.* **103**, 093602 (2009).